Research Article

Modeling and Analysis of the Dynamic Response of an Off-Grid Synchronous Generator Driven Micro Hydro Power System

Waqas Ali[a*], Haroon Farooq[a*], Akhtar Rasool[b], Intisar A. Sajjad[c], Cui Zhenhua[d], Lin Ning[d]

[a]*Dept. of Electrical Engineering (RCET Campus), University of Engineering and Technology, Lahore, Pakistan*

[b]*Dept. of Electrical Engineering, Sharif College of Engineering and Technology, Lahore, Pakistan*

[c]*Dept. of Electrical Engineering, University of Engineering and Technology, Taxila, Pakistan*

[d]*Hangzhou Regional Center (HRC) for Small Hydro Power, National Research Institute for Rural Electrification, Ministry of Water Resources, People's Republic of China*

ABSTRACT. This paper models and analyses the dynamic response of a synchronous generator driven off-grid micro hydro power system using Simulink tool of MATLAB software. The results are assessed from various perspectives including regulation through no load to full load and overload scenarios under normal and abnormal operating conditions. The investigation under the normal conditions of no load, linearly changing load and full load divulges that the system operates in a satisfactory manner as generator voltage and frequency remain approximately constant at 1 pu. However, at full load generator voltage and frequency drop 3% and 0.5% respectively from its nominal values but remain within prescribed standard IEC limits. The results also expose that the abnormal conditions produced by abrupt changes in load, system faults and severe overload, cause the unwonted variations in the magnitude of generator parameters. Moreover, the study reveals that the system stability significantly enhances when the system is run at full load because the regulation time to fix the variations in the generator parameters; except input mechanical power; decreases, e.g. from 4.1 sec to 0.8 sec for generator voltage, with the increase in the loading from quarter to full load respectively at unity power factor. Further, it is also observed that the regulation time rises, e.g. from 0.8 sec to 1.3 sec for generator voltage, with the reduction in load power factor from unity to 0.8, respectively. Thus, proper protection, to cater for increased fault current at full load and power factor correction must be provided to improve the system stability and protection. Furthermore, it is also concluded that the over loading in any case should be strongly avoided in this type of system and it should never be allowed to exceed 20% of the full load value to avoid system failure.

Keywords: Micro Hydro Power, Off-grid, No Load, Full Load, Overload, Normal, Abnormal, Response, Regulation, Modeling, Simulation

1. Introduction

Out of 7.795 billion people in the world (Sohani and Hoseinzadeh *et al.*, 2021), still 840 million people have no access to electricity (World Bank, 2019) in which 87 percent currently are living in isolated and rural settlements. The electricity coverage gap among rural and urban areas in many parts of the world (United Nation, 2019) reveals that the pace of electrification to rural communities has remained painfully slow. This is because attention is usually paid to urban regions, rather than the rural communities. Consequently, most people residing in rural areas are backward in social and economic aspects (Akinyele *et al.*, 2013; Akinyele *et al.*, 2014). The foremost reason of this energy access gap between rural and urban regions, is that it is uneconomical to extend electricity grid infrastructure to remote communities owing to the low density of population (Akinyele *et al.*, 2015). Nowadays, energy is considered as the most determining factor of humans' wellbeing (Kyriakopoulos *et al.*, 2018). Therefore, some of the people living in the rural areas rely on diesel and petrol generators to fulfil their energy needs (Umar and Hussain, 2014). But this option is not only environmentally unfriendly, but also expensive to run (Mnassri and Leger, 2010; Woodruff, 2007). These factors, coupled with the desire to improve people's living conditions in rural areas due to the inaccessibility to electricity, instigate the development of energy generation systems of localized nature. Electricity production locally as near as to the consumption site using off-grid or stand-alone power plants through renewable energy resources such as hydro, solar, wind etc. is considered the most appropriate way to provide reliable, clean and affordable energy to remote communities (Brown, 2011).

[*]Corresponding authors: Waqas Ali, waqas.ali@uet.edu.pk; Haroon Farooq, haroon.farooq@uet.edu.pk

Amongst all sources of renewable energy, hydro power is the most beneficial source and has negligible social and environmental impact, compared to other renewable energy forms (Arabatzis and Kyriakopoulos *et al.*, 2017). Micro hydro is a type of hydroelectric power that typically generates from 5 kW to 100 kW of electricity using the natural flow of water (Hoseinzadeh *et al.*, 2020). It is the low cost, small size and can be installed to serve a small community making its implementation more appropriate in the socio-political and environmental context (Nasir, 2013). Micro hydro power (MHP) systems are usually run-of-river systems which require very small flow of water with little or no requirement of water reservoir (Ali *et al.*, 2017a; Ali *et al.*, 2018a; Ali *et al.*, 2018b; Ali *et al.*, 2018c; Ali and Farooq, 2019). In addition, they have high efficiency range in between 70 to 90 percent (by far the best of all renewable energy technologies), high-capacity factor usually greater than 50 percent (in comparison to the 10% for solar and 30% for wind power plant) and less output power variations (Nasir, 2014).

For off-grid or stand-alone low power generation based upon MHP unit, the induction generator (IG) is considered more suitable than the synchronous one (Ion and Marinescu, 2013a; Ion and Marinescu, 2013b; Ion and Marinescu, 2012) because of its advantages like low price, robustness, reduced size, simple starting and synchronization, low maintenance, good response to faults and overloads and no need of external DC power supply when capacitors are used for excitation (Ion and Marinescu, 2011; Raza *et al.*, 2013). However, for the low power range of few kW, induction machines are not manufactured specifically to operate as generators thus, series induction motors are employed as generators (Smith, 2008; Ion and Marinescu, 2013c). The drawback of the IG is the lagging power factor because the machine is magnetized from the stator (Ali and Farooq, 2019; Jussi, 2006) resulting in less power availability at a given current in comparison to synchronous machine (Ali and Farooq, 2019; Reljić, 2010). In addition, it shows poor voltage and/or frequency regulations when used for the development of micro hydro power systems specifically in self-exited mode (Saket and Varshney, 2012; Singh and Tiwari, 2013; Meshram *et al.*, 2013; Scherer *et al.*, 2013; Kathirvel *et al.*, 2015). In contrast to IG, the use of synchronous generator (SG) at low power generation is very rare as it represents a high cost compared to the entire system cost; making its application, sometimes, economically unviable (Scherer *et al.*, 2013). Despite this fact, the MHP systems using SG can be considered the most consolidated one, because of the features associated with the high performance of the technologies applied on its control (Scherer *et al.*, 2013; Scherer and de Camargo, 2011; Ali *et al.*, 2017b). Therefore, the proposed study considers SG for the development of an off-grid MHP system because of its several technical advantages over IG in terms of voltage control (Scherer *et al.*, 2013; Scherer and de Camargo, 2011; Awad *et al.*, 2005).

The focus of the presented work is to examine the dynamic response of synchronous generator driven micro hydro power system working in off-grid mode under normal and abnormal operating conditions. The normal conditions considered for the investigation are no load, linearly changing load and full load. Transient disturbances due to system faults and quick changes in load and severe overload are considered as abnormal conditions in the present analysis. This paper gives the full detailed modeling of proposed off-grid MHP system deploying SG. The investigation is carried out through digital simulations from various perspectives including regulation for no load to full load and no load to overload scenarios using Simulink tool. Simulink is a MATLAB based graphical block diagramming tool. It is commonly being used as experimenting tool for modeling, simulating and analysing energy systems (Nezhad and Hoseinzadeh, 2017). It has customizable built-in blockset libraries that makes it an attractive choice for hydroelectric systems' modeling and research (Simani *et al.*, 2014; Simani *et al.*, 2017). Alternatively, DIgSILENT PowerFactory tool can also be used for hydroelectric power systems' modeling and simulations (Olulope *et al.*, 2013) but Simulink is widely used from last two decades for the non-linear dynamics research in hydro power plants (Mahmoud *et al.*, 2004; Fang *et al.*, 2008). As the alternate softwares also comply with the standards, the simulation results would be similar.

2. Micro Hydro System General Layout

The general layout of a typical micro hydro system is shown in Fig. 1. The basic components include the weir, desilting tank, penstock, turbine and generator (Michael and Jawahar, 2017). The water from the river or stream is diverted through an intake at the weir, which then enters to a desilting tank where impurities and debris are separated in it. Sometimes, a forebay tank is also located between the intake and penstock to store the water to maintain the constant head (Ali *et al.*, 2018b). Then, water from the forebay tank is conveyed to a turbine through a pipe termed as penstock. The turbine converts the potential energy of the water into mechanical energy and the produced mechanical energy by the turbine is then converted into electrical energy with the help of a generator.

Theoretically, the hydraulic power (P_{hyd}) available from a micro hydro source is determined using the following mathematical relation (Ali *et al.*, 2018a; Ali and Farooq, 2019).

$$P_{hyd} = \rho.g.Q.H \qquad (1)$$

Where ρ, g, Q and H represent water density, gravitational constant, effective flow rate and head, respectively.
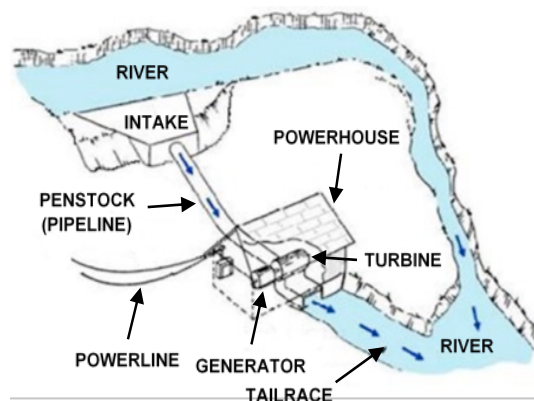

Fig. 1 General layout of a typical MHP system

This hydraulic power is normally reduced by the efficiencies of the system's components including the turbine and generator. When the hydraulic power in (1) is multiplied by overall efficiency (η) of an MHP unit, gives the final output electrical power P (Ali and Farooq, 2019):

$$P = \eta . \rho . g . Q . H \tag{2}$$

3. Methodology

3.1 System Formation and Specifications

Fig. 2 depicts the formation of proposed off-grid MHP system, taken into consideration for dynamic analysis. A variable speed micro hydro turbine drives the DC excitation based synchronous generator of 400 V, 85 kVA capacity. The electrical power generated by the SG is then distributed to sparsely scattered load through a short power line network.

3.2 System Modeling with its Components

The comprehensive model considered in this paper for the modeling and analysis of proposed MHP system, is illustrated in Fig. 3. The SG is driven by variable speed MHP turbine and is connected to off-grid load through a power line. A speed governor is used to control the speed of the micro hydro turbine. The field voltage of the DC exciter is controlled by a regulator so as to supply the balanced power to varying load. The detailed mathematical representation of all the components used in this model is discussed in the subsequent sections.

3.2.1 Modeling of Hydraulic Turbine with a Penstock

Mathematically, a penstock pipe of length L and cross-sectional area A is expressed in equation as (IEEE Working Group, 1992):

$$\frac{dQ}{dt} = (H_o - H - H_l)\frac{gA}{L} \tag{3}$$

Where H_o and H_l are static head and head loss in penstock, respectively. For rated power output, the per unit representation of (3) is given using base flow (q_{base}) and base head (h_{base}):

$$\frac{dq}{dt} = (1 - h - h_l)\frac{gAh_{base}}{Lq_{base}} \tag{4}$$

Where q, h and h_l represent per unit value of Q, H and H_l, respectively. The (4) can also be represented with water time constant. While the water time constant (T_w) is mathematically expressed as (IEEE Working Group, 1992):

$$T_w = \frac{Lq_{base}}{gAh_{base}} \tag{5}$$

Therefore, the (4) becomes as:

$$\frac{dq}{dt} = \frac{(1 - h - h_l)}{T_w} \tag{6}$$

The hydraulic turbine is basically represented by its hydraulic characteristics and output mechanical power. The per unit flow rate through the turbine is given by (IEEE Working Group, 1992):

$$q = G\sqrt{h} \tag{7}$$

Where G in (7) represents the gate position or opening. From a micro hydro source, the produced mechanical power by a turbine is the product of water effective flow rate and rated head, but this power is decreased by a factor, to account for the turbine losses. Another important factor i.e., speed deviation damping effect $DG\Delta\omega$, must also be included. Therefore, the turbine mechanical power (P_m) in per unit form is represented mathematically as (Ali and Farooq, 2019):

$$P_m = A_t h(q - q_{nl}) - DG\Delta\omega \tag{8}$$

Where A_t, q_{nl}, D and $\Delta\omega$ represent turbine gain, per unit no load flow, damping coefficient and speed deviation, respectively.

The turbine gain is calculated mathematically using full load (G_{fl}) and no load (G_{nl}) gate positions as (Kundur, 1994):

$$A_t = \frac{1}{G_{fl} - G_{nl}} \tag{9}$$

The model of a hydraulic system with a turbine and a penstock having unrestricted head and tail race is shown in Fig. 4, which is obtained by combining the (6) for the penstock, and (7) and (8) for the turbine.
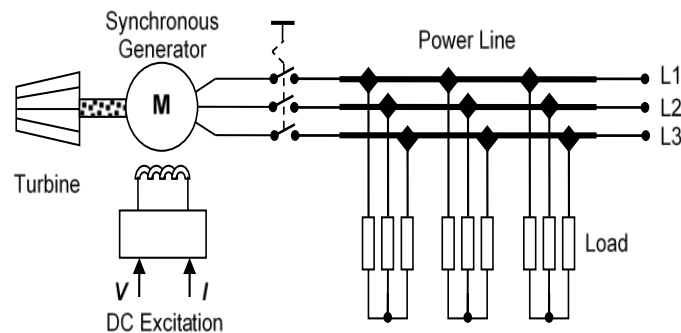

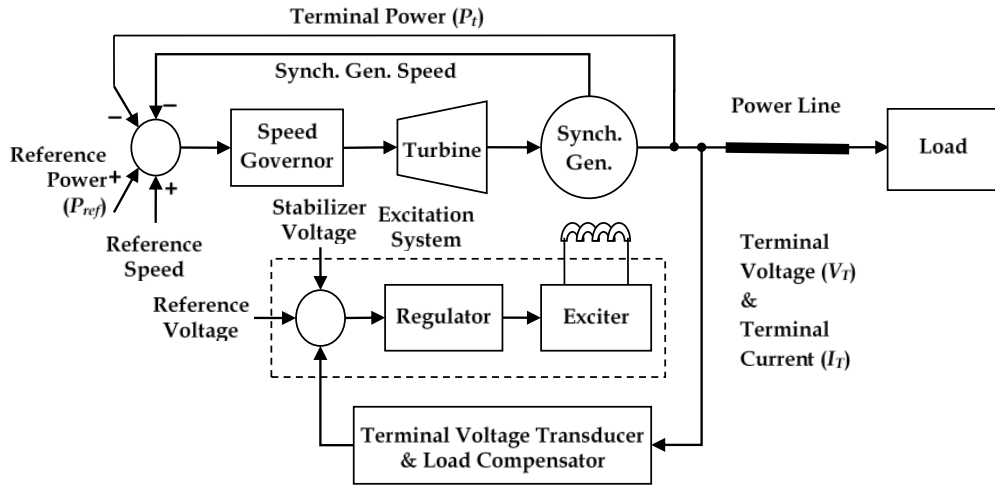**Fig. 2** Proposed off-grid MHP system formation

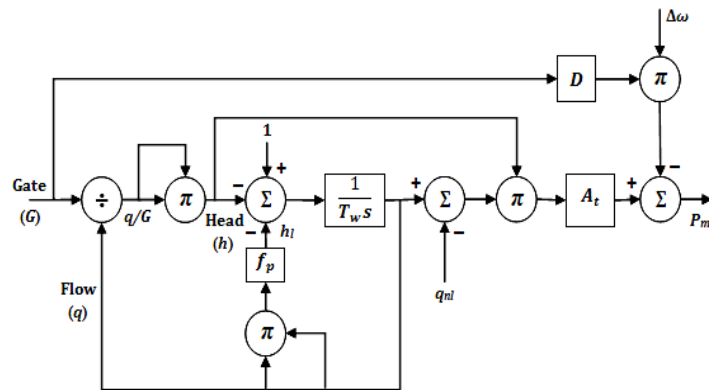**Fig. 3** Proposed MHP system's comprehensive model

Fig. 4 Penstock-turbine mathematical model (Ali and Farooq, 2019)

3.2.2 Modeling of Synchronous Generator

The modeling of synchronous generator is represented mathematically by expressing its electrical and mechanical characteristics. Using dq-axis transformation in the rotor reference frame, the machine's electrical part is represented. The equations of flux and voltage in this frame of reference are given as (Ahsan, 2013).
The flux equations:

$$\varphi_d = L_d i_d + L_{md}(i'_{fd} + i'_{kd}) \tag{10}$$

$$\varphi_q = L_q i_q + L_{mq}(i'_{kq1} + i'_{kq2}) \tag{11}$$

$$\varphi'_{fd} = L_{md}(i_d + i'_{kd}) + i'_{fd}(L'_{lfd} + L_{md}) \tag{12}$$

$$\varphi'_{kd} = L_{md}(i_d + i'_{fd}) + i'_{kd}(L'_{lkd} + L_{md}) \tag{13}$$

$$\varphi'_{kq1} = L_{mq}(i_q + i'_{kq2}) + i'_{kq1}(L'_{lkq1} + L_{mq}) \tag{14}$$

$$\varphi'_{kq2} = L_{mq}(i_q + i'_{kq1}) + i'_{kq2}(L'_{lkq2} + L_{mq}) \tag{15}$$

The equations of voltage:

$$v_d = r_s i_d - \omega_r \varphi_q + \frac{d}{dt}\varphi_d \tag{16}$$

$$v_q = r_s i_q + \omega_r \varphi_d + \frac{d}{dt}\varphi_q \tag{17}$$

$$v'_{fd} = r'_{fd} i'_{fd} + \frac{d}{dt}\varphi'_{fd} \tag{18}$$

$$v'_{kd} = r'_{kd} i'_{kd} + \frac{d}{dt}\varphi'_{kd} \tag{19}$$

$$v'_{kq1} = r'_{kq1} i'_{kq1} + \frac{d}{dt}\varphi'_{kq1} \tag{20}$$

$$v'_{kq2} = r'_{kq2} i'_{kq2} + \frac{d}{dt}\varphi'_{kq2} \tag{21}$$

Where quantities φ, L, i, v, r and ω from (10) to (21) represent the flux linkage, inductance, current, voltage, resistance and speed, respectively. In these quantities d-axis, q-axis, d-axis field, d-axis magnetizing, q-axis magnetizing, stator and rotor components are represented by the subscripts d, q, fd, md, mq, s and r, respectively. Whereas kd, $kq1$ and $kq2$ subscripts represent the dq-axis components of damper winding. While dq-axis damper winding and d-axis field winding leakage components are specified by the subscripts lkd, $lkq1$, $lkq2$ and lfd, respectively.
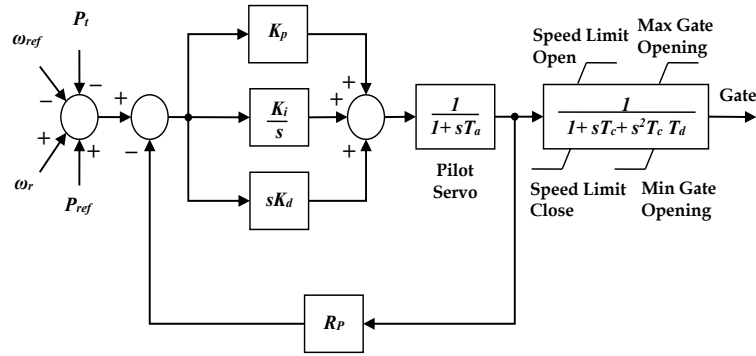
Fig. 5 Electro-hydraulic type PID speed governor's mathematical model (AL Jowder, 2013)
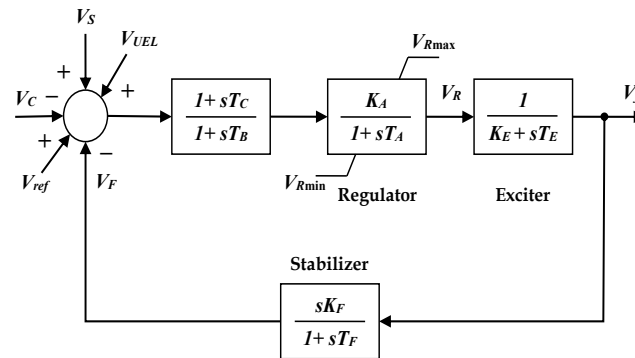

Fig. 6 Mathematical model of DC excitation system (Ali and Farooq, 2019)

The mechanical part of the synchronous machine is mathematically represented by using equation of motion of the rotor as (Ahsan, 2013):

$$\frac{d\omega_r}{dt} = \frac{1}{J}(T_m - T_e - F\omega_r) \tag{22}$$

Where T_m and T_e are the mechanical and electromagnetic torques respectively, ω_r is the speed of rotor, J is the coefficient of inertia, and F represents the friction coefficient.

3.2.3 Modeling of Speed Governor

The electro-hydraulic type PID speed governor is used for the proposed system as it is flexible and offers better performance (Ali and Farooq, 2019). Fig. 5 indicates the mathematical model of such type of speed governing system.

The proportional-integral-derivative controller's gains K_p, K_i, and K_d are chosen as per following relationships (IEEE Working Group, 1992):

$$R_T = \frac{1}{K_p} = 0.625\frac{T_w}{H} \tag{23}$$

$$T_R = \frac{K_p}{K_i} = 3.33T_w \tag{24}$$

$$\frac{K_p}{K_d} > \frac{3}{T_w} \tag{25}$$

While the values of governor time constants T_a, T_c and T_d

are set by the pressure/flow properties of the gate and its servos (Choo, 2007). The R_T and T_R in (23) and (24) represent the transient droop and reset time, respectively.

3.2.4 Modeling of Excitation System

DC based excitation system is used for synchronous generator in the proposed off-grid micro hydro power system. Fig. 6 demonstrates the mathematical model of such excitation system whose basic components are a voltage stabilizer, a voltage regulator and a DC exciter (Ali and Farooq, 2019). Amongst voltage regulator time constants T_A, T_B, T_C; T_A is the key constant while others are normally small enough to be ignored (Ali and Farooq, 2019; IEEE Std 421.5-2005, 2006).

The field voltage (V_f) at the output of exciter is mathematically related to regulator output voltage (V_R) as (IEEE Std 421.5-2005, 2006):

$$V_f = \frac{V_R}{K_E + sT_E} \tag{26}$$

Where, T_E is the exciter time constant and K_E represents the constant related to exciter self-excitation.

3.2.5 Modeling of Terminal Voltage Transducer and Load Compensator

Fig. 7 gives the mathematical model of terminal voltage transducer and load compensator model, adopted from (IEEE Std 421.5-2005, 2006). The prime input to the regulator of DC excitation system is the output voltage V_C from this model.
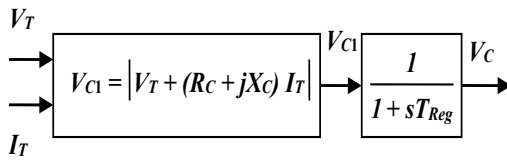
Fig. 7 Mathematical model of terminal voltage transducer and load compensator (IEEE Std 421.5-2005, 2006)

3.2.6 Modeling of Remaining Components

The remaining components of the proposed system such as power line and load are modeled using built in block-sets of SimPowerSystems library of Simulink tool of MATLAB software.

4. Results

The proposed system model is simulated to test and to analyse the dynamic response of the SG driven off-grid MHP system from various perspectives including regulation under steady and transient states at various load changing scenarios from no load to full load and from no load to overload during normal and abnormal operating conditions. The normal conditions taken for the investigation are no load, linearly changing load and full load, while the abnormal conditions include the transient disturbances due to quick changes in load and the faults on the system, and severe overload. The response of the system is depicted in waveforms for the magnitude of generator current (Ig), magnitude of generator voltage (Vg), magnitude of generator frequency (fg) and magnitude of input mechanical power (Pm) against the magnitude of different load changing scenarios of active power (PL) and reactive power (QL), in per unit (pu) form.

4.1 Results During No Load to Full Load Scenario

System is tested through no load to full load under normal operating conditions, by varying the PL (active load power) at unity power factor by keeping the QL (reactive load power) equal to zero. The simulation is carried out for 60 seconds as depicted in Fig. 8. In the start, the generator is brought into motion without connecting the load i.e., machine is running at no load. The governor maintains the nominal speed, while excitation system adjusts the field voltage so that the generator produces nominal voltage at the nominal frequency. Thus, after attaining the nominal voltage and frequency, the load can be connected to SG. During no load to full load test, the QL is maintained to 0 pu, whereas only PL is varied from 0 pu (no load) to its maximum value of 1 pu (full load).

4.2 Results During No load to Overload Scenario

System simulation is carried out for 90 sec through no load to overload to test its performance from regulation viewpoint because of the transient disturbances due to rapid load changes and system faults. The results of this testing are shown in Fig. 9. Load changes are introduced at 10 sec, 30 sec and 50 sec through the combination of PL and QL as these are the inputs to generator. The generator is started with no load i.e., both PL and QL are zero,

during this period, the SG produces nominal voltage (1 pu) at nominal frequency (1 pu). However, in the beginning when the machine starts, these parameters vary around the respective nominal values and then stabilize rapidly because of the control action of excitation and governor in MHP system. After achieving the nominal voltage and frequency, the load can be applied to SG. Therefore, at 10 sec PL increases to the half of its full load (1 pu), correspondingly QL increases to one-fourth (0.25 pu) of its full load (1 pu) at 30 sec such that the load power factor (PF) becomes 0.9. Congruently, at 50 sec PL raises to full load while QL increases to three-fourth (0.75 pu) of its nominal full load value, which reduces the PF of load to 0.8 from unity. While the transient instabilities due to faults are created at 20 sec, 40 sec and 65 sec on a 400 V line for 0.1 sec by a three-phase to ground fault. However, to examine the behaviour of the system during overload, from 80 sec onward the load on the system is successively raised from its full load value (1 pu).

5. Discussions

5.1 Response Under Normal Operating Conditions

Under normal operating conditions, the simulation results of Fig. 8 indicate that the system remains stable and operates satisfactorily as Vg and fg maintain 1 pu value as the load increased linearly from no load to full load. However; at full load there is a slight decline of 3% and 0.5% in Vg and fg respectively which should not be a major issue considering the operation of system in isolated mode where synchronization with the grid is not reqired. In addition, these deviations in voltage and frequency are within the allowable limits of IEC standards (Nömm *et al.*, 2018).

5.2 Response Under Abnormal Operating Conditions

5.2.1 System's Response During Quick Changes in Load

The results of Fig. 9 reveal that the rapid changes in load (PL or/and QL) at 10 sec, 30 sec and 50 sec produce transients in the generator voltage, frequency and current which are regulated by the control actions of the MHP system. Further, it can also be seen in the waveforms that the generator voltage and frequency slightly fall from the respective nominal value during the steady state period at full load with 0.8 PF. Whereas, the input mechanical power also drops at the occurrence of these transients caused by rapid changes in load and then varies close to its nominal value in order to adjust the output electrical power to meet the load changes or demand.

5.2.2 System's Response During Faults

The simulation results of Fig. 9 also describe the dynamic response of the system under the abnormal condition of transient disturbances caused by a three-phase to ground fault at 20 sec, 40 sec and 65 sec when the system is running in steady state. The occurrence of faults on power line causes the generator current to rise very high as depicted in the third graph of Ig and the magnitude of this fault current becomes very high for the transient that occurs when the MHP system is feeding the large load.
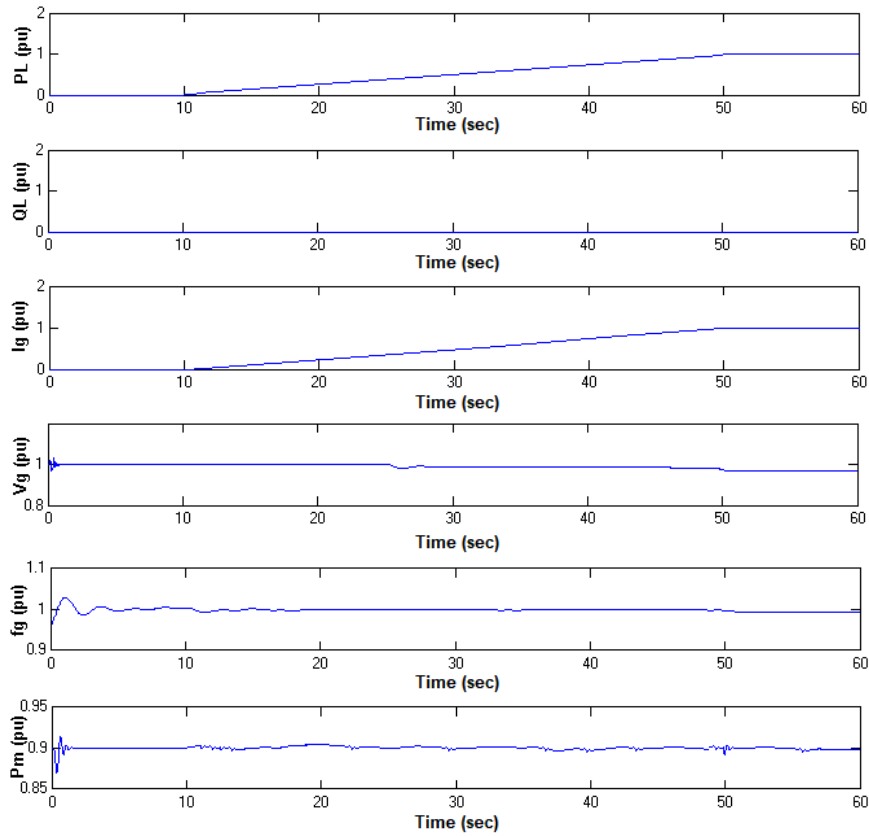
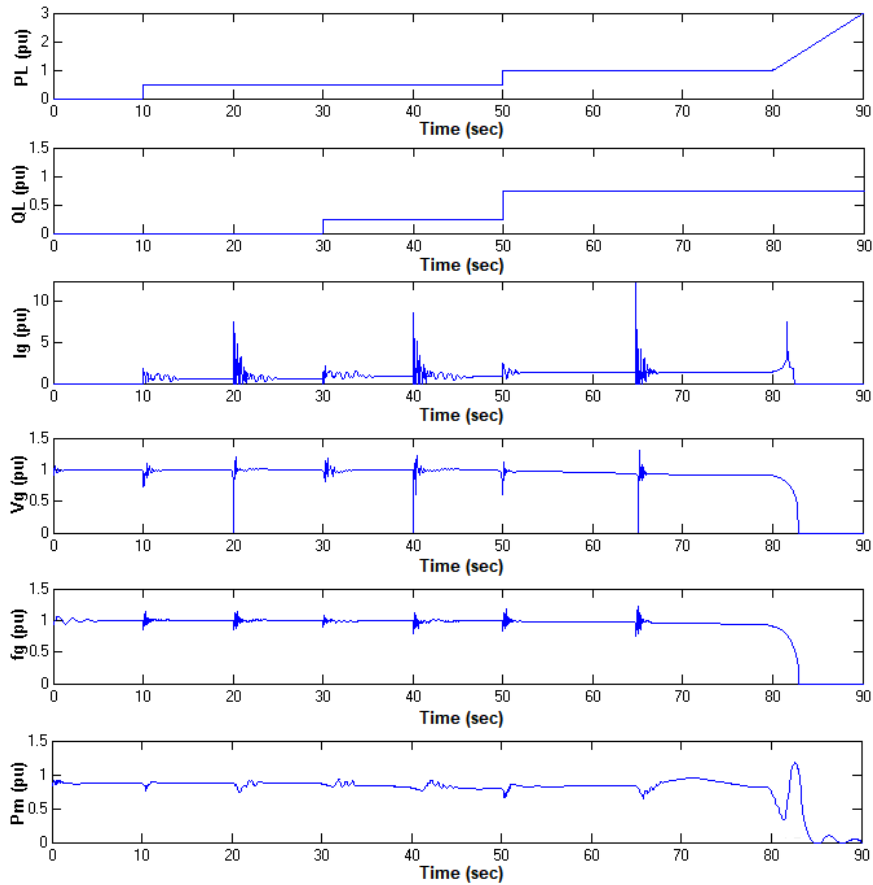**Fig. 8** System's response under normal conditions during no load to full load scenario

Fig. 9 System's response under abnormal conditions during no load to overload scenario
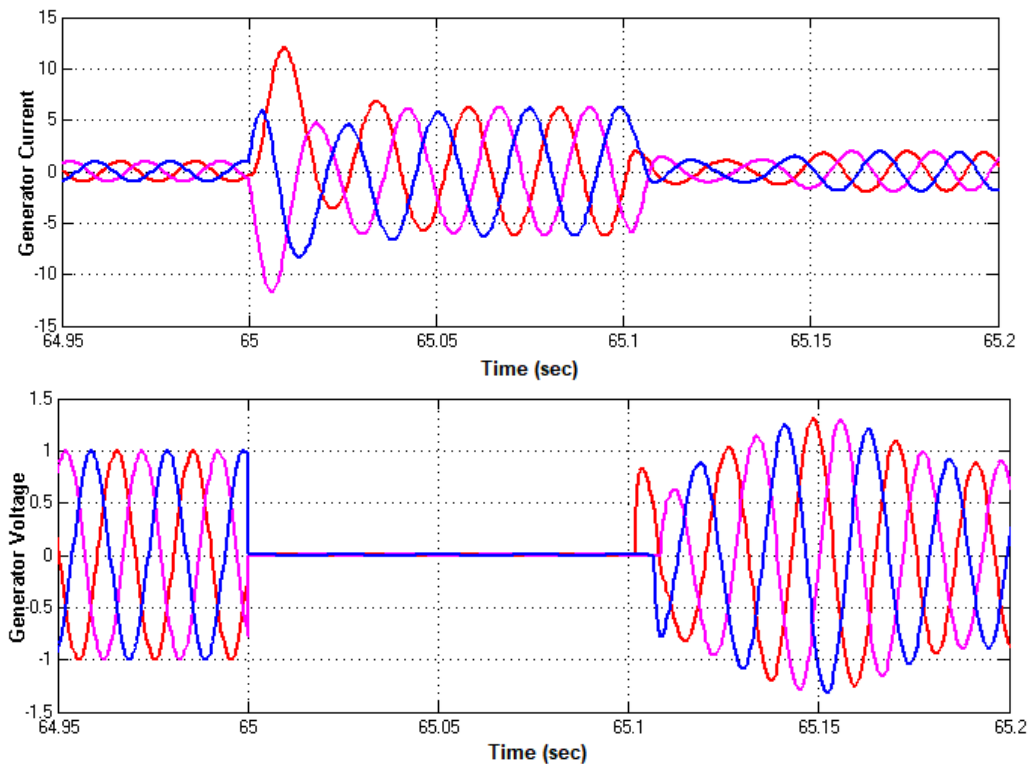
Fig. 10 Variations in the three-phase generator current and voltage from their nominal steady state values during the fault transient at 65 sec at full load

Fig. 10 depicts this state of high rise in current during fault transient at 65 sec when the system is supplying power to full load. Moreover, the graph of Vg in Fig. 9 illustrates that on the fault occurrence, the generator voltage drops to 0 pu and quickly restores to its steady state value as the fault is cleared and this situation is also shown in Fig. 10 at the incidence of transient at 65 sec. The rapid restoration of the generator voltage is because of the field voltage of excitation system that is controlled by a regulator to maintain the nominal voltage of generator. Besides, the frequency of the generator also falls on the occurrence of fault as shown in the graph of fg and then it oscillates around its nominal value of 1.0 pu as the speed governing system of MHP system normalizes it after the fault clearance. Whereas the graph of Pm in Fig. 9 indicates that the input mechanical power shows a decline before the clearing of fault and then varies increasingly to reach toward its steady state value.

5.2.3 System's Response During Overload

The waveforms of Fig. 9 also depict the results of simulation under abnormal condition of overload at 80 sec which expose that the MHP system cannot maintain the voltage and frequency, if the load is increased above its nominal full load value i.e., 1 pu. The first graph of PL shows the load increment in ramp fashion from 80 sec ahead. When the load active power crosses 1.2 pu, the generator current increases abruptly, and the voltage and frequency go down speedily, and at this time the input mechanical power takes a dip and then rises to balance the increasing load but again immediately drops to 0 pu and the system finally collapses.

5.2.4 System's Regulation Response During Transients

The graphs of Fig. 9 also show that the respective regulation time to stabilize the generator current, generator voltage and generator frequency and input mechanical power is relatively much high for fault transients as compared to transients caused by load changes, as recorded in Table 1. Moreover, the regulation time for these parameters decreases with the increase in loading on the MHP system, while the input mechanical power shows the contrary behaviour to this. However, the regulation time for these parameters increases at load with lower PF as compared to the same load with unity PF. Furthermore, the Ig, Vg and fg graphs in Fig. 9 also divulge that upon transient the generator current takes much longer time to become steady as compared to generator voltage and frequency. The time of regulation for transient disturbances caused by system faults under various simulation scenarios at different loading conditions are summarized in the Table 2 which shows that the recovery time for Ig, Vg and fg decrease with the increase in the loading except Pm. However, the magnitude of the fault current increases with the rise in loading on the MHP system as discussed already.

6. Conclusions and Future Research

6.1 Technical Findings and Suggestions

This investigation finds that the MHP system works satisfactorily and in a stable fashion under the normal operating conditions.

Table 1
Regulation time for transients caused by sudden changes in load and system faults

Parameter	Regulation Time (sec) for Transients Caused by Sudden Changes in Load			Regulation Time (sec) for Transients Caused by System Faults		
	at 0.8 PF	at 0.9 PF	at Unity PF	at 0.8 PF	at 0.9 PF	at Unity PF
Generator Current	2	5.4	3.8	2.4	6.8	5
Generator Voltage	1.8	3	2	1.3	5.6	4.1
Generator Frequency	2.2	3.8	3.1	2	5	3.6
Input Mechanical Power	4	3.5	1.7	12	5.2	3.3

Table 2
Regulation time for transient disturbances caused by system faults at different loadings

Parameter	Nominal Value (pu)		Regulation Time (sec) at Quarter Load			Regulation Time (sec) at Half Load			Regulation Time (sec) at Full Load		
	at No Load	at Full Load	at 0.8 PF	at 0.9 PF	at Unity PF	at 0.8 PF	at 0.9 PF	at Unity PF	at 0.8 PF	at 0.9 PF	at Unity PF
Generator Current	0	1	8.2	6.8	5	3.1	3.7	4.2	2.4	2.1	1.7
Generator Voltage	1	1	6.9	5.6	4.1	2.6	2.9	3.3	1.3	1	0.8
Generator Frequency	1	1	6.1	5	3.6	2	2.4	3	2	1.6	1.2
Input Power (Mechanical)	0.9	0.9	7	5.2	3.3	7.8	6.7	5.3	12	10.1	7.8

However, under abnormal operating conditions, the results depict the unwonted variations in system parameters include generator current, voltage, frequency and input mechanical power. Moreover, the respective regulation time to stabilize the generation parameteres is relatively higher for fault transients as compared to transients caused by load changes. Further, the regulation time to fix the variations in these parameters decreases with the increase in loading on the MHP system except input mechanical power that shows the contrary behaviour. Therefore, it is suggested to operate the SG driven off-grid MHP system preferably at full load. However, the appropriate protection scheme against the increased fault current must be provided to protect the system as the fault current increases in this type of system with the increase in loading. In addition, the time of regulation is increased when the power factor of the connected load on the proposed MHP system decreases from unity. Hence, it is recommended to provide appropriate PF correction to confirm the lower regulation times as well as fault current. This will also ensure the decrease in the time for which fault current flows in the network enhancing system stability and protection. Furthermore, it is also concluded that the system over loading equal or above the 1.2 times of the full load can collapse the system. Therefore, it is highly advised that the over loading of the system should be avoided in any case.

6.2 Future Research and Scope

The electrical energy storage (ESS) systems are the backbone of a stand-alone renewable power generation systems, which helps to provide a secure and reliable power supply. The operation of stand-alone or off-grid renewable power generation systems without energy storage is affected highly due to intermittent nature of generation and sudden load demand fluctuations. Of all small scale ESS options, battery based storage systems are considered more efficient in terms of scalability, efficiency, lifetime, discharge time, weight and mobility of the system (Kyriakopoulos *et al.*, 2016). Thus, combining proposed MHP system with batteries or other possible ESS options suggests area for future research whose viability need to be explore under similar or different circumstances.

Nomenclature

MHP	Micro hydro power.
IG	Induction generator.
SG	Synchronous generator.
P_{hyd}	Hydraulic power, W.
ρ	Water density, 1000kg/m^3.
g	Acceleration due to gravity, 9.8m/s^2.
Q	Water flow rate, m^3/s.
H	Head at turbine admission, m.
P	Final electrical power, W.
η	Overall system efficiency.
L	Length of penstock pipe, m.
A	Penstock cross-sectional area, m^2.
H_o	Static head, m.
H_l	Head loss in penstock, m.
q	Per unit representation of Q.
h	Per unit representation of H.
h_l	Per unit representation of H_l.
h_{base}	base head, m.
q_{base}	Base flow, m^3/s.

T_w	Water time constant, sec.
G	Gate position.
D	Damping coefficient.
$\Delta\omega$	Speed deviation.
P_m	Per unit mechanical power.
A_t	Turbine gain.
q_{nl}	Per unit no load flow.
G_{fl}	Full load per unit gate opening.
G_{nl}	No load per unit gate opening.
φ_d φ_q	Stator d and q axis flux linkage, respectively.
φ'_{fd}	d axis field winding flux linkage.
i'_{fd}	d axis field current component.
φ'_{kd} φ'_{kq1} φ'_{kq2}	d and q axis damper winding flux linkage, respectively.
L'_{lkd} L'_{lkq1} L'_{lkq2}	d and q axis damper windings leakage inductances.
L_d L_q	d and q axis combined leakage and magnetizing inductances.
L_{md} L_{mq}	d and q axis magnetizing inductance.
i_d i_q	d and q axis stator current component, respectively.
L'_{lfd}	d axis field windings leakage inductance.
i'_{kd} i'_{kq1} i'_{kq2}	d and q axis damper winding currents, respectively.
v'_{kd} v'_{kq1} v'_{kq2}	d and q axis damper winding voltages, respectively.
v_d v_q	d and q axis stator voltage component.
v'_{fd}	d axis field voltage component.
r'_{fd}	d axis field winding resistance.
r_s	stator winding resistance.
r'_{kd} r'_{kq1} r'_{kq2}	d and q axis damper winding resistances, respectively.
ω_r	Electrical angular speed of rotor.
J	Co-efficient of inertia.
T_m	Mechanical torque.
T_e	Electromagnetic torque.
F	Co-efficient of friction.
ω_{ref}	Reference/nominal speed.
P_{ref}	Per unit reference mechanical power.
P_t	Per unit terminal electrical power.
K_p	Proportional gain.
K_i	Integral gain.
K_d	Derivative gain.
R_P	Permanent droop.
T_a	Pilot servo motor time constant.
T_c	Gate closing time or gate servo gain.
T_d	Gate servo motor time constant.
R_T	Transient droop.
T_R	Reset time or dashpot time constant.
V_C	Output of terminal voltage transducer and load compensation elements.
V_{ref}	Voltage regulator reference voltage.
V_S	Power system stabilizing voltage.
V_F	Excitation stabilizer output voltage.
V_{UEL}	Underexcitation limiter output.
K_A	Voltage regulator gain.
T_E	Exciter time constant.

T_A T_B T_C	Voltage regulator time constants.
V_R V_{Rmin} V_{Rmax}	Voltage regulator output, minimum and maximum voltage regulator outputs, respectively.
K_E	Exciter constant related to self-excited field.
V_f	Exciter output voltage.
K_F	Excitation control system stabilizer gain.
T_F	Excitation stabilizer time constant.
V_T	Terminal voltage.
I_T	Terminal current.
R_C	Load compensation resistive component.
X_C	Load compensation reactance component.
V_{C1}	Compensated terminal voltage.
T_{Reg}	Regulator input filter time constant.
PL	Per unit load active power.
QL	Per unit load reactive power.
Ig	Per unit generator current.
Vg	Per unit generator voltage.
fg	Per unit generator frequency.
Pm	Per unit input mechanical power.
PF	Power factor
ESS	Electrical energy storage

References

Ahshan, R., Iqbal, M.T., Mann G.K.I., & Quaicoe, J.E. (2013, April). Modeling and analysis of a micro-grid system powered by renewable energy sources. The Open Renewable Energy Journal, 6(1), 7-22.

Akinyele, D.O., & Rayudu, R.K. (2013). Distributed power generation for energy poor-households: the Nigerian perspective. In Proc of IEEE PES Asia-Pacific Power and Energy Engineering Conference, Kowloon, China (pp. 1–6).

Akinyele, D.O., Rayudu, R.K., Nair, N.K.C., & Chakrabarti, B. (2014). Decentralized energy Generation for End-Use Applications: economic, social and environmental benefits assessment. In Proc of IEEE Innovative Smart Grid Technologies - Asia, Kuala Lumpur, Malaysia (pp. 84-89).

Akinyele, D.O., Rayuda, R.K., & Nair, N.K.C. (2015). Development of photovoltaic power plant for remote residential applications: the socio-technical and economic perspectives. Applied Energy, 155(2015), 131–149.

AL Jowder, F.A.R. (2013). Influence of Speed Governors of Hydropower Stations on Frequency Stabilization of Fixed-Speed Wind Farm. International Journal of Emerging Electric Power Systems, 14(2), 189–198.

Ali, W., Farooq, H., Rehman, A., & Farrag, M.E. (2017a). Modeling and performance analysis of micro-hydro generation controls considering power system stability. In Proc of 1st Int. Conf. on Latest trends in Electrical Engineering and Computing Technologies, Karachi, Pakistan.

Ali, W., Farooq, H., Abbas, W., Usama, M., & Bashir, A. (2017b). PID vs PI control of speed governor for synchronous generator based grid connected micro hydro power plant. Journal of Faculty of Engineering & Technology, 24(1), 53-62.

Ali, W., Usama, M., Iqbal, H., Bashir, A., & Farooq, H. (2018a). Analyzing the impact of grid connected distributed micro-hydro generation under various fault conditions. In Proc of 5th Int. Conf. on Electrical Engineering, Lahore, Pakistan.

Ali, W., Farooq, H., Usama, M., Bashir, A., & Rehman, A. (2018b). Integrating micro hydro electric power schemes into grid systems: review of barriers, procedures, requirements and problems. In Proc of 2nd Int. Conf. on Energy Systems for Sustainable Development, Lahore, Pakistan.

Ali, W., Farooq, H., Rehman, A., Jamil, M., Awais, Q., & Ali, M. (2018c). Grid interconnection of micro hydro power plants:

major requirements, key issues and challenges. In Proc. of Int. Symposium on Recent Advances on Electrical Engineering, Islamabad, Pakistan.

Ali, W., & Farooq, H. (2019). Modeling and Analysis of the Dynamic Performance of a Gird Connected Micro Hydro Power Plant Deploying Synchronous Generator. Pak. Journal of Engg. & Appl. Sciences., 24(Jan 2019), 66-78.

Arabatzis, G., Kyriakopoulos, G., & Tsialis, P. (2017). Typology of regional units based on RES plants: The case of Greece. Renewable and Sustainable Energy Reviews, 78, 1424-1434.

Awad, H., Wadi, M., & Hamdi, E. (2005). A self-excited synchronous generator for small hydro applications. In Proc: IASME/ WSEAS Int. Conf. Energy, Environment, Ecosystems and Sustainable Development, Athens, Greece (pp. 1-5).

Brown, S.V., Nderitu, D.G., Preckel, P.V., Gotham, D.J., & Allen, B.W. (2011). Renewable Power Opportunities for Rural Communities. United States Department of Agriculture (USDA). Retrieved from: https://www.usda.gov/oce/reports/energy/RenewablePowerOpportunities-Final.pdf

Choo, Y.C., Muttaqi, K.M., & Negnevitsky, M. (2007). Modeling of hydraulic governor – turbine for control stabilization. Australian and New Zealand Industrial and Applied Mathematics Journal: ANZIAMJ, 49, C681-C698.

Fang, H., Chen, L., Dlakavu, N., & Shen Z. (2008). Basic Modeling and Simulation Tool for Analysis of Hydraulic Transients in Hydroelectric Power Plants. IEEE Transactions on Energy Conversion, 23(3), 834-841.

Hoseinzadeh, S., Ghasemi, M.H., & Heyns, S. (2020). Application of hybrid systems in solution of low power generation at hot seasons for micro hydro systems. Renewable Energy, 160, 323-332.

IEEE Working Group on Prime Mover and Energy Supply Models for System Dynamic Performance Studies. (1992). Hydraulic turbine and turbine control models for system dynamic studies. IEEE Trans. on Power Systems, 7(1), 167-179.

IEEE Std 421.5-2005. (2006, April). IEEE recommended practice for excitation system models for power system stability studies. Page(s): 1 - 93

Ion, C.P., & Marinescu, C. (2011). Autonomous micro hydro power plant with induction generator. Renewable Energy, 36(8), 2259-2267.

Ion, C.P., & Marinescu, C. (2012). Hydro turbine emulator for micro hydro power plants. In Proc of Conferință Națională de Acționări Electrice, Suceava, România (pp. 143-148).

Ion, C.P., & Marinescu, C. (2013a). Stand-alone micro-hydro power plant with induction generator supplying single phase loads. Journal of Renewable and Sustainable Energy, 5(1), 1-12.

Ion, C.P., & Marinescu, C. (2013b). Micro hydro power plant with three-phase induction generator feeding single-phase consumers. In Proc of 4th International Conference on Power Engineering, Energy and Electrical Drives, Renewable Energy, Istanbul, Turkey (pp. 1211-1216).

Ion, C.P., & Marinescu, C. (2013c). Autonomous three-phase induction generator supplying unbalanced loads. Advances in Electrical and Computer Engineering, 13(2), 85-90.

Jussi, P. (2006). Induction motor versus permanent magnet synchronous motor in motion control applications: a comparative study. DSc/PhD. thesis, Lappeenranta University of Technology, Lappeenranta, Finland.

Kathirvel, C., Porkumaran, K., & Jaganathan, S. (2015). Design and implementation of improved electronic load controller for self-excited induction generator for rural electrification. The Scientific World Journal, 2015, 8 pages.

Kundur, P. (1994). Power System Stability and Control. India: Tata McGraw-Hill Education.

Kyriakopoulos, G.L., & Arabatzis, G. (2016). Electrical energy storage systems in electricity generation: Energy policies, innovative technologies, and regulatory regimes. Renewable and Sustainable Energy Reviews, 56, 1044-1067.

Kyriakopoulos, G.L., Arabatzis, G., Tsialis, P., & Ioannou, K. (2018). Electricity consumption and RES plants in Greece: Typologies of regional units. Renewable Energy, 127, 134-144.

Mahmoud, M., Dutton, K., & Denman, M. (2004) Dynamical modelling and simulation of a cascaded reservoirs hydropower plant. Electr. Power Syst. Res., 70(2), 129–139.

Meshram, S., Agnihotri, G., & Gupta, S. (2013). Performance analysis of grid integrated hydro and solar based hybrid systems. Advances in Power Electronics, 2013, 7 pages.

Michael, P.A., & Jawahar, C.P. (2017). Design of 15 kW micro hydro power plant for rural electrification at Valara. Energy Procedia, 117(2017), 163-171.

Mnassri, M.E., & Leger, A.S. (2010). Stand alone photovoltaic solar power generation system: a case study for a remote location in Tunisia. In Proc of IEEE PES General Meeting, Providence, RI, USA (pp. 1–4).

Nasir, B.A. (2013). Design of Micro - Hydro - Electric Power Station. International Journal of Engineering and Advanced Technology, 2(5), 39-47.

Nasir, B.A. (2014). Design considerations of micro-hydro-electric power plant. Energy Procedia, 50(2014), 19–29.

Nezhad, M.E.Y., & Hoseinzadeh, S. (2017). Mathematical modelling and simulation of a solar water heater for an aviculture unit using MATLAB/SIMULINK. Journal of Renewable and Sustainable Energy, 9, 063702.

Nömm, J., Rönnberg, S.K., & Bollen, M.H.J. (2018). An Analysis of Frequency Variations and its Implications on Connected Equipment for a Nanogrid during Islanded Operation. Energies, 11, 2456.

Olulope, P.K., Folly, K.A., & Venayagamoorthy, G.K. (2013). Modeling and simulation of hybrid distributed generation and its impact on transient stability of power system. In IEEE Int. Conf. on Industrial Technology, Cape Town, South Africa.

Raza, A., Xu, D., Mian, M.S., & Ahmed, J. (2013). A micro hydro power plant for distributed generation using municipal water waste with archimedes screw. In Proc of 16th International Multi Topic Conference, Lahore, Pakistan (pp. 66-71).

Reljić, D., Čorba, Z., & Dumnić, B. (2010). Application of permanent magnet synchronous generators within small-scale hydropower systems. Journal on Processing and Energy in Agriculture, 14(3), 149-152.

Saket R.K., & Varshney, L. (2012). Self excited induction generator and municipal waste water based micro hydro power generation system. Int. Journal of Engineering and Technology, 4(3), 282-287.

Scherer, L.G., & de Camargo, R.F. (2011). Advances in the modelling and control of micro hydro power stations with induction generators. In Proc: 3rd IEEE Energy Conversion Congress and Exposition, Phoenix, AZ, USA (pp. 997-1004).

Scherer, L.G., Franchi, C.M., & de Camargo, R.F. (2013). Advances in the modelling and control of micro hydro power stations applied on self-excited induction generators based on hydraulic turbine nonlinear model. Material and Processes for Energy: Communicating Current Research and Technological Developments, Formatex Research Centre, 1, 604-616.

Simani, S., Alvisi, S., & Venturini, M. (2014). Study of the Time Response of a Simulated Hydroelectric System. Journal of Physics: Conference Series, 570(Control Applications), 1-13.

Simani, S., Alvisi, S., & Venturini, M. (2017). Overview of Modelling and Control Strategies for Wind Turbines and Hydroelectric Systems: Comparisons and Contrasts. Preprints 2017, 2017080034 (doi: 10.20944/preprints201708.0034.v1).

Singh, S., & Tiwari, A.N. (2013). Voltage and frequency controller for self excited induction generator in micro hydro power plant: review. Int. Journal of Advanced Research in Electronics and Communication Engineering, 2(2), 214-219.

Smith, N. (2008). Motors as generators for micro-hydro power. London: Intermediate Technology Development Group Publishing.

Sohani, A., Hoseinzadeh, S., & Berenjkar, K. (2021). Experimental analysis of innovative designs for solar still desalination technologies; An in-depth technical and economic assessment. Journal of Energy Storage, 33, 101862.

Umar, M., & Hussain, A. (2014). Micro Hydro Power: A source of Sustainable Energy in Rural Communities: Economic and

Environmental Perspectives. Pakistan Society of Development Economists 30th AGM & Conference: Poverty, Inequality and Economic Growth, Islamabad (pp. 1-34).

United Nations. (2019). SDGs: 7 Affordable and Clean Energy - Ensure access to affordable, reliable, sustainable and modern energy for all. Retrieved from: https://unstats.un.org/sdgs/report/2019/goal-07/

Woodruff, A. (2007). An economic assessment of renewable energy options for rural electrification in Pacific Island countries.

Pacific Islands Applied Geoscience Commission (SOPAC), Technical Report 397. Retrieved from: http://www.globalislands.net/userfiles/CKIslandspdf2.pdf

World Bank. (2019). More People Have Access to Electricity Than Ever Before, but World Is Falling Short of Sustainable Energy Goals. Retrieved from: https://www.worldbank.org/en/news/press-release/2019/05/22/tracking-sdg7-the-energy-progress-report-2019